Renewable Energy Focus 53 (2025) 100685

Contents lists available at ScienceDirect

Renewable Energy Focus

journal homepage: www.elsevier.com/locate/ref

# Optimal control strategy for enhancing energy efficiency of Pelamis wave energy converter: a Simulink-based simulation approach

Alireza Vakili [a], Ali Pourzangbar [b,*], Mir Mohammad Ettefagh [c], Maghsoud Abdollahi Haghghi [d,e]

[a] Department of Engineering, University College of Nabi Akram, Tabriz, Iran
[b] Institute for Water and Environment (IWU), Karlsruhe Institute of Technology (KIT), Karlsruhe, Germany
[c] Faculty of Mechanical Engineering, University of Tabriz, Tabriz, Iran
[d] Department of Mechanical Engineering, School of Engineering, Urmia University, Urmia, Iran
[e] Department of Mechanical Engineering, Elm-o-Fann University College of Science and Technology, Urmia, Iran

ARTICLE INFO

*Keywords:*
Ocean wave energy
Power Take-Off (PTO)
Wave energy converter
Pelamis
Optimal control

ABSTRACT

Wave energy is a promising renewable resource due to its predictability, consistency, and low environmental impact, making it an efficient solution for electricity generation in marine environments. Among various wave energy converters, the Pelamis stands out for its simplicity and scalability; however, its energy conversion efficiency can be further improved through advanced control strategies. This research aims to enhance the energy extraction efficiency of a Pelamis wave energy converter by implementing an optimal control strategy to regulate the production torque within the power take-off (PTO) system between the Pelamis cylinders. A dynamic model of the system interacting with regular waves is developed, and optimal control theory is applied to compute the PTO torques in real-time, maximizing the energy captured. The Pelamis energy converter and its control system were simulated in MATLAB's Simulink environment. The results indicate that applying the optimal control method leads to a threefold increase in energy capture compared to the Proportional-Integral-Derivative (PID) control approach and a tenfold increase compared to the uncontrolled system. Additionally, frequency analysis of the average power output demonstrates that the energy gain with the optimal controller is achieved across all wave frequencies.

## 1. Introduction

Wave energy captures the immense power of ocean waves to produce electricity by transforming the kinetic and potential energy generated by waves into mechanical energy, which is subsequently converted into electrical energy using [1]. One key benefit of wave energy is its reliability; unlike wind and solar energies, ocean wave patterns can be accurately [2]. Furthermore, wave energy installations generally have a smaller environmental footprint, occupying less land than solar and wind farms [3]. They also enhance energy security by augmenting the energy sources available, representing a viable and eco-friendly option for addressing the rising global energy needs while helping to combat climate change [4]. This also can make wave energy a cost-effective solution for generating electricity in the marine environment [5].

There are several methods for extracting energy from ocean waves, including wave energy converters (WECs) such as Pelamis, wave-induced pressure systems, wave energy buoys, and the Wave Dragon [6]. These WECs demonstrate various methods for extracting wave energy, illustrating the potential to develop sustainable energy solutions that utilize the natural dynamics of our oceans, making a significant contribution to the global renewable energy landscape [7].

Pelamis is considered an attractive option for wave energy generation because it is relatively simple in design and can be easily scaled up or down depending on the location and the wave energy resource [8]. Additionally, it is relatively low-cost and low-maintenance and can be placed in various water depths [9]. One advantage of Pelamis over other wave energy converters is that Pelamis is an attenuator device, meaning it extracts energy through the relative motion of its articulated segments. This absorption method allows for more efficient energy conversion without relying on fixed frames and seabed construction [10]. The efficiency of the Pelamis is influenced by a number of parameters,

* Corresponding author at: Institute for Water and Environment (IWU), Karlsruhe Institute of Technology (KIT), Karlsruhe, Germany
*E-mail addresses:* Vakili.meceng@yahoo.com (A. Vakili), ali.pourzangbar@kit.edu (A. Pourzangbar), ettefagh@tabrizu.ac.ir (M.M. Ettefagh), st_m.abdollahihaghi@urmia.ac.ir (M. Abdollahi Haghghi).

https://doi.org/10.1016/j.ref.2025.100685
Received 2 January 2025; Received in revised form 10 February 2025; Accepted 10 February 2025
Available online 11 February 2025

**Nomenclature**

| | |
|---|---|
| $a_j$ | Acceleration of body oscillation on waves (m/s$^2$) |
| $a_n$ | Two-dimensional added-mass coefficient (-) |
| $a_n\dot{w}_r$ | Hydrostatic force required to accelerate the added mass (N) |
| $a_x$ | Added mass (kg) |
| $A$ | Wave amplitude (m) |
| $A_{33}$ | Added-mass coefficient in the heave direction (-) |
| $A_{55}$ | Added-mass coefficient in the Pitch direction (-) |
| $A_r$ | System matrix (-) |
| $A_{wp}$ | Wet surface area of a floating object (m$^2$) |
| $b_1$ | Damping coefficient (-) |
| $b_n$ | Two-dimensional damping coefficient (-) |
| $b_n w_r$ | Hydrostatic damping force (N) |
| $B_{33}$ | Rotational damping coefficient in heave direction (N.m.s/rad) |
| $B_{55}$ | Rotational damping coefficient in the Pitch direction (N.m.s/rad) |
| $B_r$ | Input matrix (-) |
| $c_n\chi_r$ | Hydrostatic force generated by Relative displacement (N) |
| $d$ | Water depth (m) |
| $e^{-k}$ | Pressure reduction coefficient (-) |
| $E_r$ | Output matrix (-) |
| $F$ | Force applied on a floating body (N) |
| $F_P$ | Configuration matrix (-) |
| $GM_t$ | Metacentric height (m) |
| $H$ | Hamiltonian function (-) |
| $I_{ww}$ | Moment of inertia of each cylinder cross section (kg.m$^2$) |
| $J$ | Cost Function (-) |
| $K$ | Wave number (m$^{-1}$) |
| $L$ | Length of the floating object (m) |
| $m$ | Mass of the floating object (kg) |
| $m_n\ddot{x}_n$ | Force required to accelerate the mass (N) |
| $M$ | Excitation torque (N.m) |
| $M_0$ | Amplitude of excitation torque in pitch direction (N.m) |
| $M_{pitch}$ | Hydrostatic moment (N.m) |
| $n$ | A vector perpendicular to the surface of the floating body (-) |
| $P$ | Excitation moment range in the pitch direction (Pa) |
| $Q$ | Forces and moments applied on the hull of a floating object by waves (-) |
| $T$ | Wave period (S) |
| $u$ | Velocity of the floating object (m/s) |
| $U$ | Input of control system or torque generated by PTO systems (-) |
| $U_j$ | Oscillation speed of the body on the waves (m/s) |
| $\dot{w}_r$ | Acceleration of each point on the floating object relative to the sea surface (m/s$^2$) |
| $X_r$ | Independent state variables (-) |
| $x_r$ | Relative displacement of each point on the floating object and sea surface (m) |
| $\dot{x}$ | Velocity in the heave direction (m/s) |

*Greek symbols*

| | |
|---|---|
| $\gamma$ | Oscillation of the floating object (-) |
| $\gamma_a$ | Amplitude of oscillation of the floating object (m) |
| $\lambda$ | Wavelength (m) |
| $\lambda(t)$ | Lagrange multipliers (-) |
| $\lambda_{33}$ | Two-dimensional damping coefficient (-) |
| $\mu_{33}$ | Two-dimensional added-mass coefficient (-) |
| $\tau$ | Water height in equilibrium state (m) |
| $\vartheta_w$ | The speed of the traveling wave (m/s) |
| $\phi_A$ | Potential of hull of the floating object in interaction with waves (m$^2$/s) |
| $\phi_j$ | Potential of wave velocity (m$^2$/s) |
| $\omega$ | Frequency-domain oscillation of the floating object (-) |
| $\omega_e$ | Encounter frequency (-) |
| $\nabla_0$ | Volume of displaced water (-) |
| $\rho$ | Water density (kg/m$^3$) |
| $\Delta F_\gamma$ | Additional restoring force in heave direction (-) |

*Abbreviations*

| | |
|---|---|
| *PTO* | Power Take Off |
| *PID* | Proportional-Integral-Derivative |
| *WECs* | Wave Energy Converters |
| *OTEC* | Ocean Thermal Energy Converters |
| *LCOE* | Levelized Cost Of Energy |

including wave conditions at the deployment site, operating and maintenance access, reliability, environmental factors, and power rating [11].

Recent studies have demonstrated growing advancements in WEC technologies and control strategies, some of which are reviewed in the following. O'Connor et al. [12] presented that increasing the power rating of the Pelamis increased its efficiency, but this also increased the cost of the device. Thomson et al. [13] conducted a life cycle assessment of the Pelamis wave energy converter and identified significant environmental impacts during installation and maintenance, contributing to higher costs and its discontinuation. Johnson and Martinez [14] emphasized the environmental benefits of WECs like Pelamis. Their findings showed that these systems caused minimal ecological disturbance, making them a sustainable option for large-scale deployment in offshore environments. Ghaneei and Mahmoudi [15] presented that Pelamis performed optimally in offshore locations with high wave energy resources, where wave heights and periods were significant, and its efficiency improved with wave irregularity, performing better in irregular rather than regular waves. Ghaedi et al. [16] explored the reliability of Pelamis wave energy converters integrated into electrical networks. They employed a multi-state framework to investigate component failures and fluctuations in power output, resulting in an exergy efficiency of 85%. Through fuzzy c-means clustering, they optimized various power conditions, demonstrating that wave patterns greatly influence system reliability and contribute to improved performance. The findings were further supported by comparisons to simulations conducted via the Monte Carlo method.

As stated, the WEC is a complex system comprising various subsystems that transfer energy from the ocean to electricity [17]. The system's frequency response influences control strategies for Power Take-Off (PTO), impacting energy absorption [18]. Phase control with latching, which adjusts the phase angle of the PTO system, increases mean power [19] and proves especially useful in wave energy converters operating in irregular or changing wave conditions [20]. To improve the efficiency of wave energy absorption, de Falcão [21] presented a straightforward strategy and algorithm for the phase control of a point absorber in irregular, random waves through the utilization of the latching technique. Ni et al. [22] presented that to optimize the performance and cost-effectiveness of the Pelamis wave energy converter, significant attention was directed toward improving the efficiency of its power conversion system and control mechanisms. Nizamani et al. [23] stated that investigating the hydrodynamic characteristics and also the power generation capacity of Pelamis using numerical simulations in the time-frequency response domain as well as methods developed based on

Fourier transform proved that an adaptive control strategy could increase the power generation capacity up to 15.9%. Sheshaprasad et al. [24] conducted a time domain simulation to analyze four PTO systems using National Data Buoy Center datasets. The results indicated that the binary-reactive PTO system was the most optimal solution for the surface-riding WEC, given the constraints of limited tube length and non-sinusoidal wave patterns. Wang et al. [25] studied the impact of control strategies and wave climates on the power performance and Levelized Cost of Energy (LCOE) of wave power farms and showed that the optimal linear active control strategy reduced LCOE and improved annual energy generation compared to the passive control strategy, especially when machinery constraints were considered. de Falcão et al. [26] emphasized the importance of adaptive control strategies for optimizing energy harvesting in irregular wave conditions, which were crucial for WECs like Pelamis. Their research indicated that adaptive PTO tuning could boost efficiency by up to 20%. Mehdipour et al. [27] examined how to enhance the PTO configurations of oscillating surge WECs through the use of a new algorithm known as the Hill Climb - Explorative Grey Wolf Optimizer (HC-EGWO). This method resulted in a 3.31% improvement in power output compared to various adaptations of the grey wolf optimizer and a significant 45% increase over other optimization strategies, boosting the efficiency of oscillating surge WECs in demanding conditions. Hall et al. [28] optimized PTO systems in WECs to maximize energy capture. Their analysis compared two approaches based on model predictive control. They demonstrated that integrating hydraulic dynamics into PTO could lead to a 23% increase in power output during irregular wave situations, emphasizing the critical role of effective control mechanisms in tapping ocean energy. Shao et al. [29] focused on optimizing PTO systems within WECs, indicating their vital importance for energy-harnessing efficiency. They compared four complex models, assessing power performance across six sea states for the WEC. The findings indicated that each modeling technique had benefits and limitations, suggesting customized strategies for various simulation goals. Ali et al. [30] explored the PTO configurations of subsurface WECs to maximize energy capture. Their analysis revealed that a three-PTO configuration significantly improved broadband performance and power quality while effectively harnessing energy across all degrees of freedom, with only minor gains observed with additional PTOs.

According to the literature review, many studies have consistently demonstrated the efficacy of utilizing PTO control in a WEC; however, to our best knowledge, very little attention has been paid to the modeling and control of the PTO system in Pelamis wave energy converters. Hence, to respond to this gap, this study aims to boost the energy output of the Pelamis wave energy converter by using an optimal control approach to synchronize the production between its cylinders. The method presented in this study is primarily applicable to regular wave conditions due to its open-loop control nature. While irregular waves introduce challenges such as unknown external disturbances, the findings of this research provide a foundation for improving energy conversion efficiency in controlled environments. To achieve this, we analyzed the energy absorption under three PTO system conditions: no control, Proportional-Integral-Derivative (PID) control, and optimal control. Different techniques, including experimental [31] and numerical [32–33] methods, are used to investigate the impact of PTO control on the converted energy. Numerical models created in Simulink, a reliable and cost-effective tool, have been widely utilized in various studies [34–35]. Hence, Simulink is employed as a graphical programming platform for modeling, simulating, and examining dynamic systems in this research.

The structure of this paper is organized into four distinct main sections to enhance clarity and readability and present the research and findings. The Introduction (first section) provides essential background information and outlines the primary research objectives. Following this, the materials and methods section (second section) details the procedures used in the research, including ocean wave and Pelamis converter specifications (subsection 2.1), Pelamis dynamic modeling (subsection 2.2), state space for the dynamic's equations of the Pelamis converter (subsection 2.3), control strategies, involving optimal control design for the Pelamis energy converter and control law extraction (subsection 2.4), and Simulink (subsection 2.5). This section also provides details on the optimization and analysis of the study. The results and discussion section (third section) presents the study's findings derived from the simulation of the Pelamis with an optimal control system (subsection 3.1), simulation of the Pelamis with an PID control system (subsection 3.2), and comparison of Pelamis performance in controlled and uncontrolled conditions (subsection 3.3). Finally, the conclusion section (fourth section) summarizes the main findings, uncertainties, limitations, and suggests areas for future research.

## 2. Material and methods

### 2.1. Ocean wave and Pelamis converter specifications

Wind-generated waves are not regular and have a random nature. However, most methods for analyzing and designing offshore structures are based on regular waves. In fact, regular wave theories approximate the actual wave conditions in a way that is satisfactory for most engineering purposes [36]. Accordingly, this study assumes regular wave conditions for simplicity, though real ocean waves are irregular with varying amplitudes, frequencies, and directions. Regular waves are chosen instead of irregular or random waves to provide a controlled and repeatable environment for optimal control strategy, allowing for a clear assessment of the system's dynamic response while minimizing uncertainties. This approach establishes a baseline understanding of the Pelamis wave converter's behavior, ensures comparability with prior research [37–38], and enhances computational feasibility by avoiding the complexities of stochastic wave variability, making the analysis more interpretable and efficient. Future research should incorporate irregular wave models and address factors like actuator limitations, environmental variability, and system degradation to enhance the applicability of the control strategy.

Table 1 lists the necessary parameters for simulating ocean waves and transforming energy into electricity [37]. The wave conditions considered in this study were carefully selected to align with the assumptions of Airy wave theory, which requires that the ratio of wave height ($H$) to wavelength ($\lambda$) be much smaller than 1 ($H/\lambda \ll 1.0$). Based on the parameters in Table 1, the wavelength was calculated using the dispersion relation, yielding $\lambda = 22.38\,m$. The resulting ratio $H/\lambda = 0.089$ confirms that the wave conditions are well within the linearity range, validating the use of Airy wave theory in this analysis.

A regular and harmonic wave is used first to start a transformer simulation. Then, if an answer is obtained in this environment, an irregular and random wave and actual conditions are used for the subsequent stages. Accordingly, we assumed that the waves impacting the Pelamis are harmonic and consistent. Hence, the ocean waves can be depicted as regular waves through Eq. (1).

**Table 1**
Specifications of the wave used in this study

| Parameter | Value | Unit |
|---|---|---|
| Wave amplitude (half the wave height) | 1 | m |
| Wave period | 3.8 | s |
| Water depth | 10 | m |
| Water density | 1000 | $Kg/m^3$ |
| Pelamis Volume | 6.95 | $m^3$ |
| Length of each Pelamis cylinder | 6.8 | m |
| Pelamis mass | 1102.27 | Kg |
| Moment of Inertia | 4463.43 | $Kg.m^2$ |
| Depth of bouncy | 0.33 | m |
| Rotational damping coefficient of connecting damper | 1.04E06 | $N.m.s/rad$ |
| Stiffness factor of connecting spring | 9.0E05 | $N.m/rad$ |

$$\eta = \frac{H}{2}\sin(kx - \omega t) \tag{1}$$

In which $\gamma$ is the free surface elevation at time+ t and horizontal position $x$, $H$ is the wave height, $k = 2\pi/L$ is the wave number, $L$ is the wavelength, $\omega = 2\pi/T$ is wave angular frequency, and $T$ wave period. In this study, the water depth ($d$) is 10 m (shallow water), so the wavelength will be obtained from Eq. (2).

$$L = T\sqrt{gd} \tag{2}$$

### 2.2. Pelamis dynamic modeling

Fig. 1 illustrates the connection of the pendulum cylinders in the Pelamis, which are connected by 4 cylinders through 3 hydraulic PTO systems. The hydraulic PTO system is designed and controlled in such a way as to generate only pure torsional moments. Furthermore, the bottom panel of Fig. 1 shows each cylinder's free vibration diagram. The external moment generated by the PTO system affects the behavior of each cylinder, which is considered in the dynamic equations of each cylinder.

The moment created in every PTO system is a function of relative angular velocity and displacement between cylinders and the performance of control manifolds. The dynamic equations of each cylinder are as follows:

Cylinder 1

$$\begin{aligned}(m + a_z)\ddot{x} + b_1\dot{x} + c_1x + d\ddot{\theta} + e\dot{\theta} + h\theta = F_1(t)\\ (I_{ww} + A_{ww})\ddot{\theta} + B\dot{\theta} + C\theta + D\ddot{x} + E\dot{x} + Hx = M_1(t) + M_{PTO,1}\end{aligned} \tag{3}$$

Cylinder 2

$$\begin{aligned}(m + a_z)\ddot{x} + b_1\dot{x} + c_1x + d\ddot{\theta} + e\dot{\theta} + h\theta = F_2(t)\\ (I_{ww} + A_{ww})\ddot{\theta} + B\dot{\theta} + C\theta + D\ddot{x} + E\dot{x} + Hx = M_2(t) - M_{PTO,1} + M_{PTO,2}\end{aligned} \tag{4}$$

Cylinder 3

$$\begin{aligned}(m + a_z)\ddot{x} + b_1\dot{x} + c_1x + d\ddot{\theta} + e\dot{\theta} + h\theta = F_3(t)\\ (I_{ww} + A_{ww})\ddot{\theta} + B\dot{\theta} + C\theta + D\ddot{x} + E\dot{x} + Hx = M_3(t) - M_{PTO,2} + M_{PTO,3}\end{aligned} \tag{5}$$

Cylinder 4

$$\begin{aligned}(m + a_z)\ddot{x} + b_1\dot{x} + c_1x + d\ddot{\theta} + e\dot{\theta} + h\theta = F_4(t)\\ (I_{ww} + A_{ww})\ddot{\theta} + B\dot{\theta} + C\theta + D\ddot{x} + E\dot{x} + Hx = M_3(t) + M_{PTO,3}\end{aligned} \tag{6}$$

in which $m$ is the mass of the cylinder, $a_z$ is added mass (kg), $b_1$ refers to the linear damping coefficient ($N.s/m$), $c_1$ stands for linear stiffness coefficient ($N/m$), $d$ is added rotational inertia coefficient ($kg.m^2$), $e$ is the coupling coefficient for rotational motion ($kg{\cdot}m^2/rad$), $h$ refers to linear-angular coupling coefficient ($N/rad$), $I_{ww}$ moment of inertia of the cylinder cross-section ($kg.m^2$), $A_{ww}$ is the added rotational inertia due to water in the pitch direction ($kg.m^2$), $B$ represents the rotational damping coefficient ($N.m.s/rad$), $C$ is rotational stiffness coefficient ($N{\cdot}m/rad$), $D$ is coupling coefficient for angular acceleration ($kg{\cdot}m/rad{\cdot}s^2$), $E$ stands for the coupling coefficient for linear acceleration ($kg{\cdot}m/s^2$), and $H$ refers to the external force coupling coefficient ($N$). $F_i(t)$ and $M_i(t)$ represents the external force and torque acting on the cylinder $i^{th}$, respectively. Finally, $M_{PTO}$ is torque generated by the PTO system ($N{\cdot}m$).

The connection of the Pelamis energy converter cylinders through the spherical joints means the existence of constraints. Using these constraints, the dynamic equations describe the behavior of the Pelamis energy converter. The presence of these constraints reduces the degrees of freedom of the system from 8 to 5. The constraints resulting from spherical joints and their degrees of freedom are shown in Fig. 2.

Inspection of Fig. 2 reveals that the degrees of freedom related to $x_1$, $x_2$, and $x_3$ are dependent on the degrees of freedom ($\theta_1$, $\theta_2$, $\theta_3$) as described below.

$$x_2 = x_1 + \frac{l}{2}\theta_1 + \frac{l}{2}\theta_2 \tag{7}$$

$$x_3 = x_1 + \frac{l}{2}\theta_1 + l\theta_2 + \frac{l}{2}\theta_3 \tag{8}$$

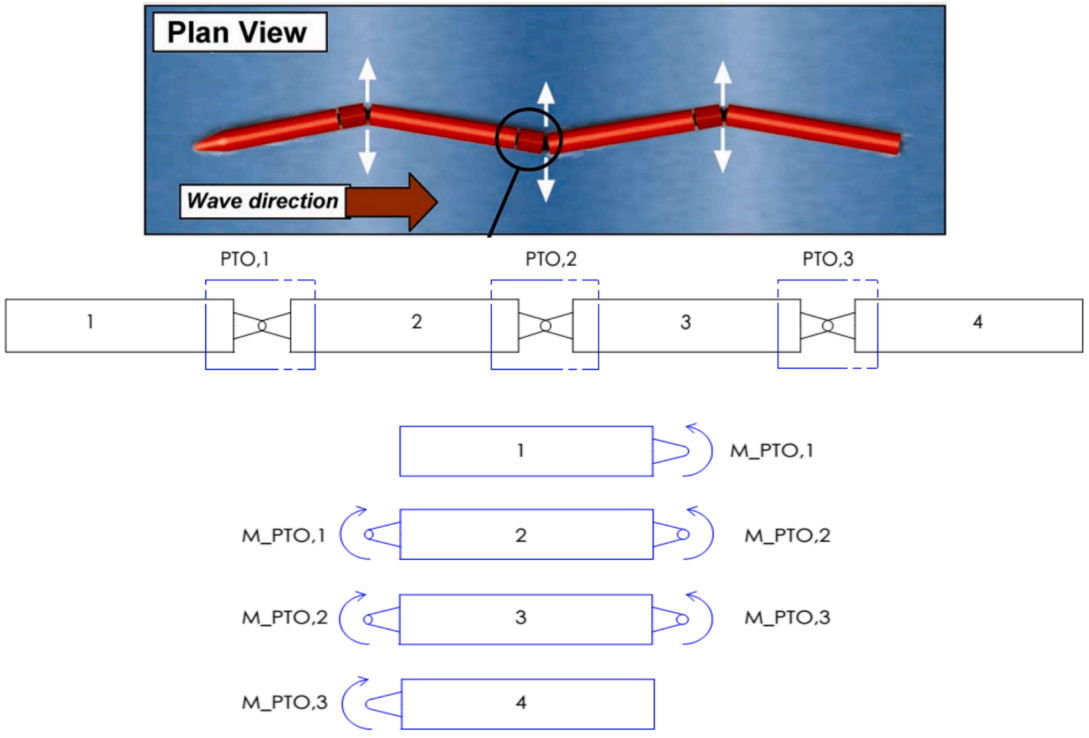


**Fig. 1.** Pelamis energy converter schematic and the free vibration diagram of its different components; Plan view (upper panel) and its cross section (middle panel); Free vibration diagram of Pelamis components (bottom panel) [37].

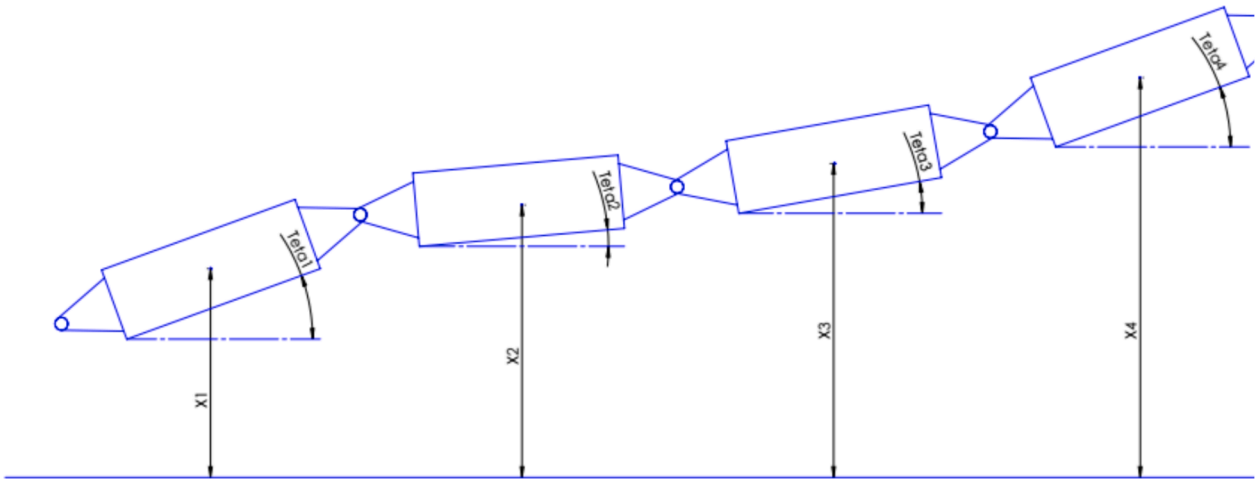


**Fig. 2.** Degrees of freedom of the Pelamis energy converter [37].

$$x_4 = x_1 + \frac{l}{2}\theta_1 + l\theta_2 + l\theta_3 + \frac{l}{2}\theta_4 \tag{9}$$

### 2.3. State space for the dynamic's equations of the Pelamis converter

The state variables are considered as follows to describe the dynamics of the Pelamis energy converter in state space form and the complete degree.

$$X = \begin{bmatrix} X_d & \theta & \dot{X}_d & \dot{\theta} \end{bmatrix} \tag{10}$$

in which $X_d = [x_1 \quad x_2 \quad x_3 \quad x_4]$ and $\theta = [\theta_1 \quad \theta_2 \quad \theta_3 \quad \theta_4]$.

Considering the linearity of Eqs. (3) to (6), the state space model of the Pelamis is presented in the following form:

$$\dot{X} = AX + BU + EQ \tag{11}$$

where $Q$ represents the moments and forces that waves apply to the Pelamis cylinders, and $U$ is the control input, the same as the generated moment from the PTO system. $A$ is the system matrix, and $B$ is the control system input matrix. Eq. (11) and constraints 7 to 9 represent the complete state-space model for the Pelamis energy converter.

It is recommended that the reduced order state space model be used in the control systems design. This model will express the dependent state variables as the independent state variables. The independent state variables are selected as $X_r = \begin{bmatrix} x_1 & \theta & \dot{x}_1 & \dot{\theta} \end{bmatrix}$, and the transformation matrix between the full order state variables and the reduced order state variables is given by Eq. 12.

$$\begin{aligned} [X_d \quad \theta] &= P[x_1 \quad \theta] \\ \begin{bmatrix} \dot{X}_d & \dot{\theta} \end{bmatrix} &= P\begin{bmatrix} \dot{x}_1 & \dot{\theta} \end{bmatrix} \\ P &= \begin{bmatrix} 1 & 0 & 0 & 0 & 0 \\ 1 & l/2 & l/2 & 0 & 0 \\ 1 & l/2 & l & l/2 & 0 \\ 1 & l/2 & l & l & l/2 \\ 0 & 1 & 0 & 0 & 0 \\ 0 & 0 & 1 & 0 & 0 \\ 0 & 0 & 0 & 1 & 0 \\ 0 & 0 & 0 & 0 & 1 \end{bmatrix} \end{aligned} \tag{12}$$

Using this transformation, the reduced order state space model will be as follows.

$$\dot{X}_r = A_r X_r + B_r U + E_r Q \tag{13}$$

$$A_r = \begin{bmatrix} 0_{5\times5} & I_{5\times5} \\ -(P^T M P)^{-1} & -(P^T M P)^{-1}(P^T C P) \end{bmatrix} \tag{14}$$

$$B_r = \begin{bmatrix} 0_{5\times3} \\ (P^T M P)^{-1} P^T B_1 \end{bmatrix} \tag{15}$$

$$B_1 = \begin{matrix} 0_{4\times3} \\ \begin{bmatrix} 1 & 0 & 0 \\ -1 & 1 & 0 \\ 0 & -1 & 1 \\ 0 & 0 & -1 \end{bmatrix} \end{matrix} \tag{16}$$

$$E_r = \begin{bmatrix} 0_{5\times8} \\ (P^T M P)^{-1} P^T \end{bmatrix} \tag{17}$$

where $0_{m\times n}$ represents a $m \times n$ matrix of zeros and $I_{m\times n}$ is a $m \times n$ matrix of ones. The superscript "$T$" indicates the trsnpose of a matrix and superscript "-1" represents its inversion.

### 2.4. Control strategies

The most important principle for increasing the energy received from ocean wave energy conversion systems is the synchronization of the forces exerted by ocean waves and the movement of the moving parts of the energy converter. In other words, the maximum energy received from ocean waves is achieved when the wave energy converter operates under conditions close to resonance [39], meaning that the dominant wave frequency aligns with the undamped natural frequency of the PTO system. Under these conditions, resonant oscillations enhance energy absorption, but maintaining optimal performance requires adjusting PTO damping. Excessive damping restricts motion, reducing efficiency, while insufficient damping leads to suboptimal energy conversion. Therefore, continuous adaptation is necessary to keep the system near resonance under varying wave conditions. Phase control methods have been developed to control the movement phase of wave energy converters. However, due to technical difficulties in implementation, they have given way to suboptimal methods such as latching control. Although this is true for one-degree-of-freedom converters, in multi-degree-of-freedom converters, the maximum energy received does not necessarily occur under resonance conditions. Therefore, in this research, an optimal control method has been used to determine the control input, i.e., the torque applied to the structure by the PTO system.

In the proposed control structure for the Pelamis wave energy converter to increase the energy received from ocean waves, all state variables are assumed to be measurable. In addition, it is assumed that the values of the force and torque exerted by ocean waves on the structure of the Pelamis wave energy converter can be calculated based on the measured states and wave characteristics. In this structure, the forces and torques applied to the Pelamis wave energy converter by ocean waves are considered disturbances, i.e., external inputs over which we have no control. Therefore, the control system's awareness of the applied disturbances will significantly impact its performance.

A PID control system will be designed and simulated to increase the efficiency and power of the Pelamis wave energy converter and evaluate the performance of the optimal control system. Our strategy for designing the PID controller is based on the fact that in wave energy converters, the maximum power occurs in the resonance mode. Therefore, the PID controller is designed to reduce the phase difference between the force and torque of the waves and the angular displacement of the cylinders in the Pelamis wave energy converter.

#### 2.4.1. Optimal control design for the Pelamis energy converter

The cost function is introduced as the average energy received from the ocean, in accordance with Eq. (23), given that the aim of controlling the Pelamis converter is to enhance the energy acquired from ocean waves.

$$J = \frac{1}{T}\int_0^T XF_pUdt \tag{23}$$

In this equation, the state variables' vector $X$ is the vector of the control inputs $U$ (which in this case are the moment produced by the PTO system), and the configuration matrix $F_p$. It combines the input with the system states in different ways and depends on the configuration of the structure being examined. In Pelamis, given that the energy received is the product of the relative rotational velocity between the two shafts in a moment of the PTO system, the configuration matrix will be as follows (Eq. 24):

$$F_p = \begin{bmatrix} 0 & 0 & 0 \\ 0 & 0 & 0 \\ 0 & 0 & 0 \\ 0 & 0 & 0 \\ 0 & 0 & 0 \\ 0 & 0 & 0 \\ 1 & 0 & 0 \\ -1 & 1 & 0 \\ 0 & -1 & 1 \\ 0 & 0 & -1 \end{bmatrix} \tag{24}$$

The configuration matrix *Fp* defines the mapping between the PTO system's torque and the relative rotational velocities of the Pelamis joints. Since energy extraction occurs through oscillatory motion, *Fp* captures the relationship between control inputs and state variables, ensuring an accurate representation of the system's power generation mechanism. The structure of *Fp* is derived based on the system kinematics and hydrodynamic constraints, where each row corresponds to a degree of freedom influenced by the adjacent segments. The negative and positive elements indicate opposite contributions to relative motion between the connected cylinders.

In this problem, the control input must be determined such that the defined cost function reaches its maximum value. However, the optimal control problem will have a unique solution only if the Hamiltonian function is concave. Therefore, Eq. (25) is utilized as a substitute for the prior cost function, ensuring that the Hamiltonian function satisfies the requirement of concavity. In this study, the cost function is designed primarily to assess the impact of different control strategies on energy extraction efficiency. While physical constraints such as PTO torque limits and actuator saturation are not explicitly included, we acknowledge that these considerations could be incorporated in future studies to enhance real-world applicability.

$$J = \frac{1}{T}\int_0^T (XF_pU + \frac{1}{2}U^TRU)dt \tag{25}$$

In this relation, $R$ is a positive diagonal definite matrix whose elements are weighted by system inputs (Eq. 26).

$$R = \begin{bmatrix} r_1 & 0 & 0 \\ 0 & r_2 & 0 \\ 0 & 0 & r_3 \end{bmatrix} \tag{26}$$

Each diagonal element $r_i$ represents the relative importance of the corresponding control input and are tuned based on system characteristics. The weighting matrix R in Eq. (26) is selected to balance energy extraction and control effort. Since the PTO-generated moment is limited by system constraints, the diagonal elements of R are tuned to prevent excessive control forces while maintaining efficient energy conversion. Higher values of R reduce control effort but may limit energy capture, while lower values enable aggressive control at the expense of increased actuation forces. The values of $r_1, r_2, and r_3$ are determined based on system dynamics, wave frequency response, and empirical tuning, following optimal control principles [40].

Considering that the PTO generated moment is proportional to its capacity and cannot exceed a specific limit, the amount of PTO moment can also be determined by setting the matrix $R$ in the cost function introduced in Eq. (25).

#### 2.4.2. Control law extraction

In order to establish the optimal control input, the maximum value of the cost function presented in Eq. (27) must be determined. To accomplish this, we will utilize the Hamiltonian function, which is derived based on the following equation.

$$H = X^TF_pU + \frac{1}{2}U^TRU + \lambda^T(AX + BU + EQ) \tag{27}$$

In the Hamiltonian framework, the Lagrange multipliers (λ) correspond to the costate variables, which describe the sensitivity of the cost function to variations in the system states. These multipliers ensure that the optimal control law satisfies necessary conditions for energy maximization while enforcing constraints arising from the system dynamics. Physically, they can be interpreted as generalized forces or adjoint variables that drive the optimization process.

According to Pontryagin's Maximum Principle, the following conditions must hold for optimal control.

$$\dot{\lambda} = -\frac{\partial H}{\partial x} = -F_pU - A^T\lambda \tag{28}$$

$$\dot{X} = AX + BU + EQ \tag{29}$$

The optimal control law is found by differentiating the Hamiltonian with respect to $U$ and setting it to zero:

$$\frac{\partial H}{\partial U} = {F_p}^TX + RU + B^T\lambda = 0 \tag{30}$$

By simplifying the above equations, we will have:

$$U = -R^{-1}({F_p}^TX + B^T\lambda) \tag{31}$$

$$\dot{\lambda} = F_pR^{-1}{F_p}^TX + (F_pR^{-1}B^T - A^T)\lambda \tag{32}$$

$$\dot{X} = (A - BR^{-1}{F_p}^T)X + BR^{-1}B^T\lambda + EQ \tag{33}$$

As an alternative method for calculation, we assume $\lambda = KX + S$, then:

$$\dot{\lambda} = \dot{K}X + K\dot{X} + \dot{S} \tag{34}$$

By substituting Eq. (33) into Eq. (34) and simplifying, we obtain:

$$\dot{\lambda} = \dot{K}X + K\left[(A - BR^{-1}F_p{}^T)X + BR^{-1}B^T\lambda + EQ\right] + \dot{S} \quad (36)$$

From Eq. 28, we equate:

$$-F_pU - A^T\lambda = \dot{K}X + K\left[A(A - BR^{-1}F_p{}^T)X + BR^{-1}B^T\lambda + EQ\right] + \dot{S} \quad (36)$$

Substituting $\lambda = KX + S$ and Eq. (31) into Eq. (36), one obtains:

$$-F_p\left[-R^{-1}(F_p{}^TX + B^T\lambda)\right] - A^T(KX + S) = \dot{K}X + K\left[(A - BR^{-1}F_p{}^T)X + BR^{-1}B^T(KX + S) + EQ\right] + \dot{S} \quad (37)$$

By simplifying the above equation, we obtain:

$$\dot{K} = (F_pR^{-1}B^T - A^T)K - K(A - BR^{-1}F_p{}^T) - KBR^{-1}B^TK + F_pR^{-1}F_p{}^T \quad (38)$$

$$\dot{S} = (F_pR^{-1}B^T - A^T)S - KBR^{-1}B^TS - KEQ \quad (39)$$

After solving the above differential equations and determining the values of $K$ and $S$ at each moment, the control input will be calculated as follows:

$$U = -R^{-1}(F_p{}^T + B^TK)X - R^{-1}B^TS \quad (40)$$

Given that in a steady state, $\dot{k} = \dot{S} = 0$, by solving the following equations, the matrices $K$ and $S$ will be obtained as follows:

$$(F_pR^{-1}B^T - A^T)K - K(A - BR^{-1}F_p{}^T) - KBR^{-1}B^TK + F_pR^{-1}F_p{}^T = 0 \quad (41)$$

$$(F_pR^{-1}B^T - A^T)S - KBR^{-1}B^T - KEQ = 0$$

By substituting the values obtained for $K$ and S Eq. (41) and inserting the result into Eq. (40), the control input in the steady state will be obtained. The equation obtained for the control input possesses the property that the amount of control input generated can be controlled by adjusting the weighting coefficients in the matrix $R$. Detailed information are presented in Borzì [41], and Anderson and Moore [42].

### 2.5. Simulink

After dynamic modeling and obtaining the motion equations of the system, we need to simulate the system in Simulink software. The block diagram of the Pelamis wave energy converter system is presented in Appendix A for detailed reference. Fig. 3 illustrates the block diagram of the model layout, including inputs, state variables, and output variables.

The proposed control structure of the Pelamis wave energy converter aims to maximize energy extraction by optimizing the PTO system force and velocity. This approach relies on a feedforward control strategy, where predictions of wave excitation are used to dynamically adjust system parameters in real time. State feedback control is employed, assuming that all state variables are measurable, as precise knowledge of these variables is essential for effective regulation.

The control process begins with wave excitation estimation, where external forces and torques exerted by ocean waves are characterized based on measured states and wave properties. These forces are treated as external disturbances, meaning they represent inputs beyond direct control. The optimal control system determines the best PTO force and velocity setpoints by considering wave conditions, PTO damping, and stiffness coefficients. Instead of direct feedback, the feedforward controller anticipates the optimal response, maximizing energy extraction. The state variables defining system motion include the displacement, velocity, and acceleration of Pelamis cylinders, along with relative rotation, rotational speed, angular displacement, and angular acceleration. Additionally, the linear acceleration at the mass center and mass center velocity contribute to system dynamics. Following this, the Pelamis system's motion is computed, where wave forces drive the device's movement, influencing the displacement, velocity, and acceleration of the cylinders, as well as their relative rotation, rotational speed, angular displacement, and angular acceleration. The PTO system adjusts mechanical properties such as swashplate angle and excitation current to enhance power conversion, optimizing force application to maintain an optimal energy capture state. The final system response is reflected in the PTO torque, the instant and average power generated, and the total power extracted based on wave frequency, with the PID-controlled PTO system regulating the moment and energy output efficiency. Subsequently, the controller regulates PTO damping and stiffness, refining the system response to maintain energy efficiency and ensuring alignment with optimal force and velocity setpoints. The final step combines the optimal PTO force and controller adjustments, generating the final system response, ensuring that the device operates under ideal conditions for energy extraction. Ultimately, the PTO system converts mechanical motion into electrical energy, completing the energy conversion process.

## 3. Results and discussion

To demonstrate the control system's effectiveness in enhancing energy obtained from sea waves, a simulation of the Pelamis wave energy converter, along with its control systems, has been performed using MATLAB/Simulink software. Given that the primary research focuses on augmenting energy from regular waves, these waves have been generated based on the available data in Ref. [7], with the resulting forces and torques applied to the energy converter structure. To better assess the performance of the proposed control methodology, simulations were run in both controlled and uncontrolled states, with results presented accordingly. In the unchecked state, the hydraulic PTO system is modeled as an equivalent torsional spring-damper between two parts of the structure, with the hydraulic circuit valves set to specific predetermined values. Based on Eq. 2 and the information summarized in Table 1, the wave pattern in the center of each cylinder of the energy converter is illustrated in Fig. 4.

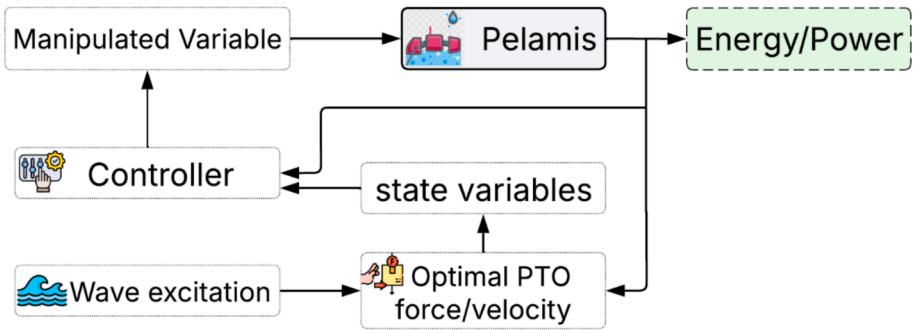


**Fig. 3.** The block diagram of the model layout, including inputs, state variables, and output variables.

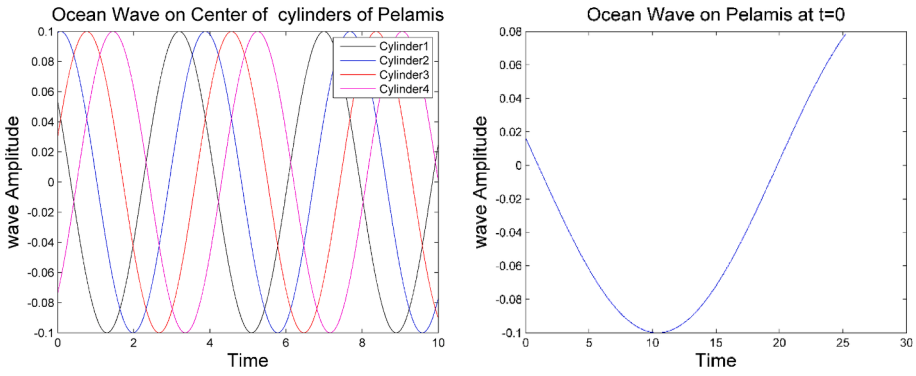


**Fig. 4.** Variation of regular wave height against time at the mass center of different cylinders (left panel); variations in wave height along the Pelamis wave energy converter (right panel).

### *3.1. Simulation of the energy conversion device of Pelamis without control system*

The upper panels of Fig. 5 illustrate the wave-induced forces (Panel A) and torques (Panel B) acting on the mass center of the Pelamis cylinders due to regular waves. These forces and torques exhibit a periodic nature, which is expected given the regular wave excitation. The observed phase difference between the forces and torques acting on different cylinders arises due to the spatial separation between the mass centers and the propagation time of the wave as it moves along the Pelamis structure. The bottom panels of Fig. 5 provide insights into the kinematics of the Pelamis system. Panel C depicts the displacement of the mass center of each cylinder over time. It can be observed that the displacements are not purely sinusoidal, suggesting that multiple wave harmonics contribute to the system's response. This is due to the structural constraints imposed by the PTO system and the coupling effects between adjacent cylinders. Panel D presents the relative angular displacement between consecutive Pelamis cylinders. The presence of multiple harmonics in these angular displacements is a direct result of the mechanical constraints linking the cylinders. The flexible joints cause each segment's motion to influence the next, leading to interdependent oscillatory behavior.

These results highlight the fundamental dynamics of the Pelamis energy converter under regular wave excitation. The phase shifts and multi-harmonic responses emphasize the importance of wave-structure interaction and mechanical coupling in determining energy conversion efficiency. A control strategy is necessary to regulate these oscillations, synchronize cylinder motion, and improve energy harvesting performance. Future sections will investigate how different control approaches influence these dynamics.

The upper panels of Fig. 6 illustrate the velocity of the Pelamis cylinder mass centers (Panel A) and their relative angular velocity (Panel B). As previously observed, the motion of each cylinder is influenced by multiple harmonics, which arise from the constraints between the

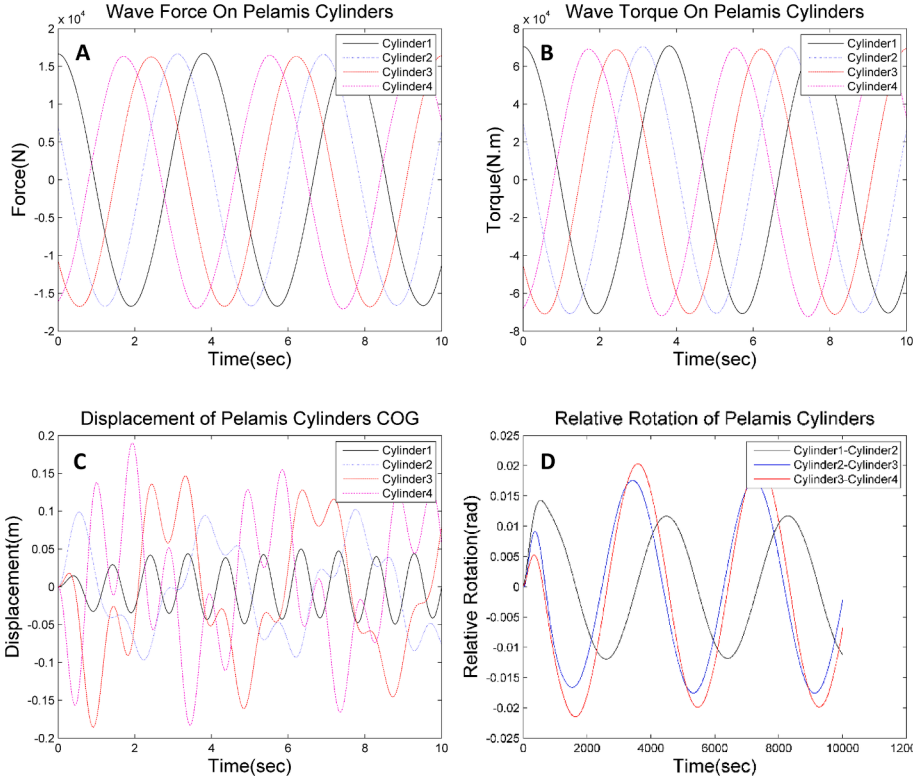


**Fig. 5.** Wave-induced force on the mass center of the Pelamis cylinders (Panel A); wave-induced torque on the mass center of Pelamis cylinders. (Panel B); Displacement of the mass center of Pelamis cylinders. (Panel C); and relative angular displacement between the Pelamis cylinders (Panel D).

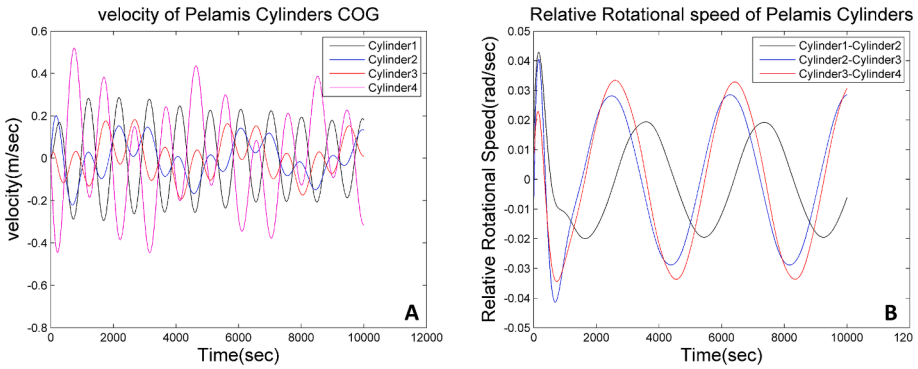


**Fig. 6.** Mass center velocity of Pelamis cylinders (Panel A); relative angular velocity of Pelamis cylinders (Panel B).

cylinders. This results in interdependent motion, where the behavior of one segment affects the response of the others. The relative angular velocity shown in Fig. 6 (Panel B) is of particular importance, as the energy conversion process in Pelamis depends on the relative motion of adjacent cylinders at the joints. The steady-state response indicates a dominant harmonic component, which suggests that wave-induced oscillations generate sustained periodic movement. The bottom panels of Fig. 7 focus on the power take-off (PTO) system. Panel A shows the PTO torque, which is directly responsible for energy extraction. The hydraulic PTO system converts this torque into hydraulic force, which then applies pressure to the hydraulic fluid, ultimately transforming mechanical energy into electrical power. Panel B presents the instantaneous power output, calculated as the product of the PTO-generated torque and the relative velocity between connected cylinders. The total power extracted by the Pelamis wave energy converter is obtained by summing the contributions from all PTO systems.

This analysis highlights the significance of relative angular velocity and PTO torque in determining power output. The observed multi-harmonic response suggests that the system's mechanical constraints and hydrodynamic interactions play a crucial role in shaping its performance. A well-designed control strategy is necessary to optimize the synchronization of PTO dynamics with wave-induced oscillations, thereby enhancing energy conversion efficiency.

The upper panels of Fig. 8 illustrate key dynamic parameters that define the motion characteristics of the Pelamis wave energy converter. Panel A presents the relative angular acceleration of Pelamis cylinders, which represents the rotational response of the system under wave-induced excitations. The behavior of this parameter is essential in evaluating the mechanical stability and energy conversion efficiency, as excessive rotational acceleration could introduce unwanted mechanical stresses or inefficiencies in the PTO system. Panel B of Fig. 8 focuses on the linear acceleration at the mass center of the Pelamis cylinders, providing insights into the overall response of the structure to external perturbations. The presence of multiple frequency components suggests a complex interplay between hydrodynamic forces and structural constraints, emphasizing the importance of optimal PTO damping to regulate acceleration levels and maximize power extraction.

The lower panels of Fig. 9 present the power generation performance of the Pelamis system across different wave frequencies. Panel A illustrates the PTO average power as a function of frequency for individual PTO units, highlighting the variation in energy absorption across different sections of the device. The peak power extraction occurs at specific frequency ranges, confirming the dependence of hydrodynamic coefficients on wave frequency. Panel B of Fig. 9 provides a system-wide perspective by summing the power contributions of all PTO units, offering a clearer understanding of the Pelamis system's optimal operating frequency range. The observed peak in total PTO power suggests that without active control, energy absorption is inherently tuned to a specific frequency dictated by the device's structural and hydrodynamic properties. The location of this peak could be adjusted by modifying system parameters or implementing advanced control strategies to enhance energy capture efficiency under varying sea conditions.

The analysis highlights the dependence of PTO power generation on wave frequency and the need for adaptive tuning strategies to optimize energy capture. Furthermore, the insights into acceleration profiles emphasize the importance of mechanical stability in maintaining efficient energy conversion. Future sections will explore the role of control strategies in addressing these challenges and enhancing system performance.

### 3.2. *Simulation of the Pelamis with an optimal control system*

The behavior of the Pelamis energy converter is analyzed in a scenario where an optimal control system actively modulates the PTO power output by dynamically adjusting the stiffness and damping coefficients via hydraulic actuators. Unlike the uncontrolled case, where these parameters remain constant, the control system enables real-time adaptation to wave conditions, optimizing energy extraction.

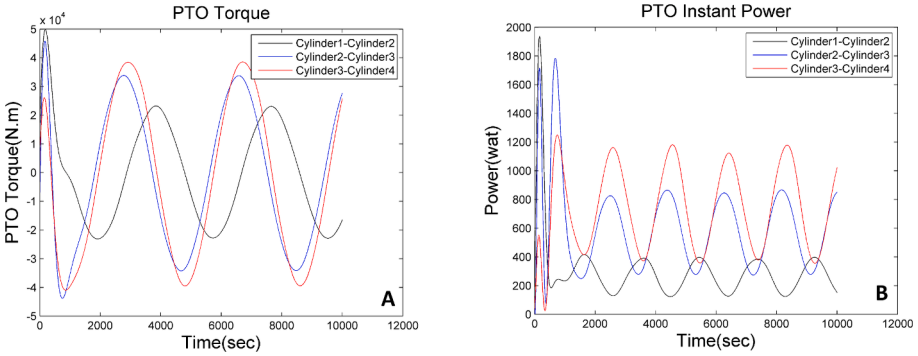


**Fig. 7.** Torque generated by PTO systems (Panel A); instant power generated by PTO systems (Panel B).

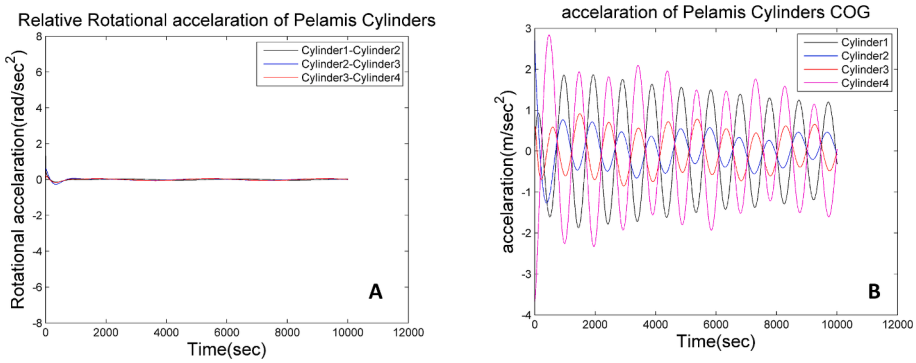


**Fig. 8.** Relative angular acceleration of Pelamis cylinders (Panel A); linear acceleration at the mass center of Pelamis cylinders (Panel B).

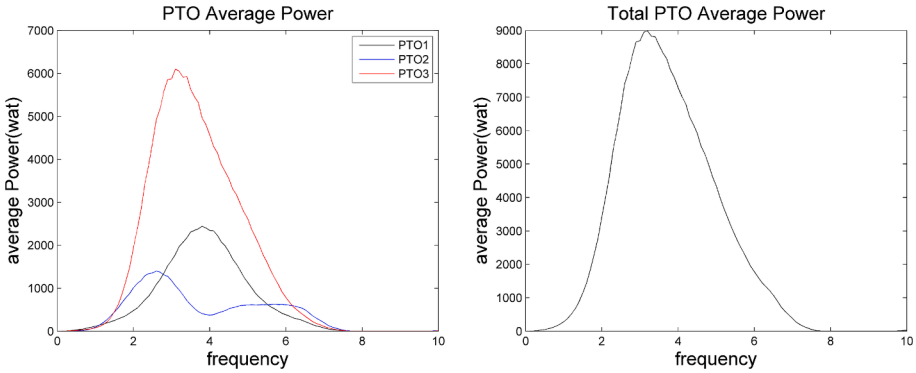


**Fig. 9.** PTO Average Power generated by the Pelamis based on wave frequency (left panel) and average total power generated by the Pelamis based on wave frequency (right panel).

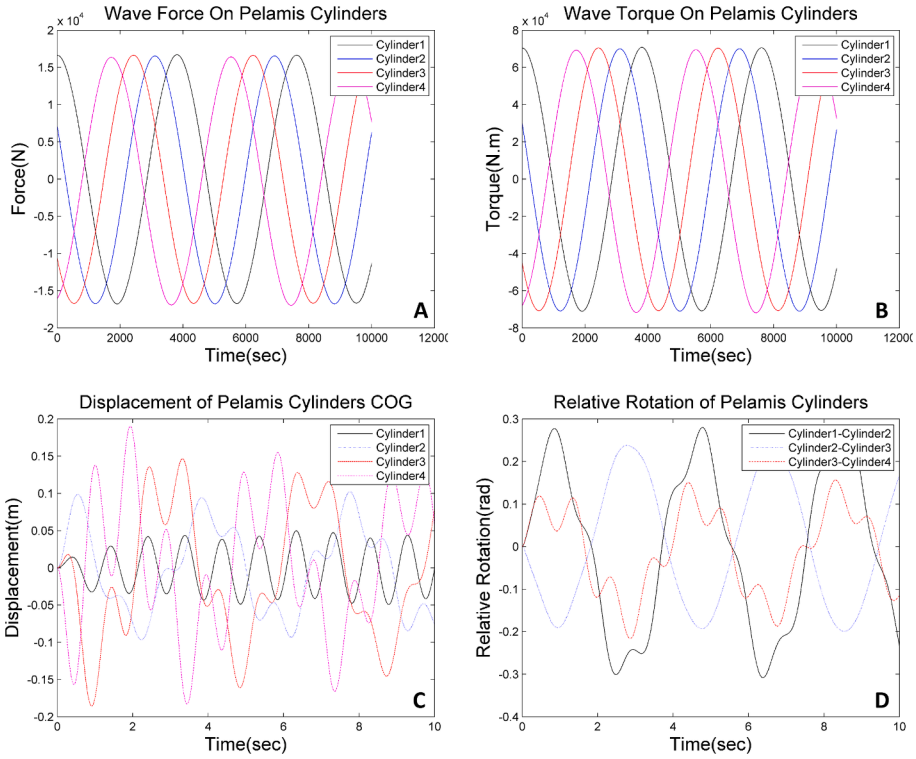


**Fig. 10.** Force applied to the Pelamis cylinders (Panel A); moment applied to the Pelamis cylinders (Panel B); displacement of the mass center of Pelamis cylinders. (Panel C); and relative angular displacement between the Pelamis cylinders (Panel D).

The upper panels of Fig. 10 illustrate the wave-induced forces (Panel A) and torques (Panel B) applied to the Pelamis cylinders. Compared to the uncontrolled case, higher amplitudes of forces and torques are observed, indicating that the control system allows greater oscillatory motion, leading to increased energy absorption from ocean waves. The lower panels of Fig. 10 depict the relative linear displacement (Panel C) and relative angular displacement (Panel D) between adjacent Pelamis cylinders. The controlled PTO system increases the amplitude of displacement variations, demonstrating that the control mechanism effectively synchronizes the motion of the cylinders with the incoming wave energy. This synchronization is essential for maximizing power conversion efficiency, as it ensures that the relative motion between the cylinders aligns with the optimal energy extraction phase.

Fig. 11 further investigates the kinematic response of the Pelamis system under optimal control. Panel A illustrates the mass center velocity of the Pelamis cylinders, showing higher amplitude oscillations compared to the uncontrolled case. This increase highlights the effectiveness of the control system in capturing more wave energy. Panel B presents the relative angular velocity between the cylinders, which is a crucial parameter for power extraction. The control system maintains well-defined oscillatory patterns, ensuring that relative motion remains within operational constraints while maximizing energy transfer.

Fig. 12 provides a direct evaluation of the power take-off (PTO) system's performance under optimal control. Panel A displays the PTO torque, which is dynamically regulated by the control system. A key observation is that the torque is generally in phase with the relative velocity between the cylinders, ensuring efficient energy conversion. However, in some instances, the control system applies an opposing torque to prevent excessive movements, thereby avoiding structural overloading and mechanical failures. Panel B illustrates the instantaneous power generated by the PTO system. Compared to the uncontrolled case (Fig. 8), a significant increase in power output is evident. This confirms that optimal control effectively utilizes the Pelamis device's full capacity, allowing it to extract more energy from ocean waves.

Fig. 13 presents additional performance metrics under optimal control. Panel A shows the relative angular acceleration of Pelamis cylinders, where the control system regulates rotational accelerations to prevent undesired mechanical stress. Panel B displays the linear acceleration at the mass center, reflecting the dynamic response of the structure under optimized energy extraction conditions. Panel C highlights the average PTO power generated at different wave frequencies, demonstrating that the control system modifies the power distribution profile compared to the uncontrolled scenario. Panel D represents the total PTO average power, where a notable increase in overall power generation is achieved due to the adaptive tuning of the PTO system.

The control system significantly enhances power extraction by synchronizing the motion of Pelamis cylinders with wave-induced forces while preventing excessive mechanical stress. Compared to the uncontrolled scenario, the introduction of dynamic PTO modulation leads to higher power output and more efficient utilization of wave energy.

### 3.3. Simulation of the Pelamis with an PID control system

Fig. 14 illustrates the forces and moments applied to the Pelamis cylinders under PID control. Panel A shows the wave-induced forces acting on different cylinders, while Panel B presents the corresponding torques. Compared to the uncontrolled case, the force and torque amplitudes are regulated, demonstrating the impact of the PID controller in modulating system response to ocean waves. By adjusting the proportional, integral, and derivative gains, the controller reduces extreme variations in forces and torques, maintaining structural stability. The lower panels (C and D) represent the displacement of the mass center and the relative angular displacement of the Pelamis cylinders. The PID control system slightly increases displacement amplitudes compared to the uncontrolled scenario, but this increase is smaller than that observed with the optimal control system. The reason is that PID controllers primarily act as passive regulators rather than energy maximizers.

Fig. 15 illustrates the effect of PID control on the dynamic response of the Pelamis cylinders. Panel A presents the velocity of the mass center, while Panel B shows the relative angular velocity between adjacent cylinders. The velocity trends confirm that the PID controller regulates wave-induced oscillations without significantly amplifying them, unlike the optimal control strategy. The observed velocities highlight the fundamental principle of wave energy conversion—maximizing oscillatory motion while maintaining stability. Since the Pelamis system generates power through relative motion between its segments, the controlled velocity ensures effective power transfer to the PTO system while mitigating extreme structural loading. Unlike open-loop control strategies, PID regulation maintains stability under varying wave conditions by dynamically adjusting the damping and stiffness coefficients of the PTO system.

Fig. 16 directly examines the power output of the Pelamis device under PID control. Panel A depicts the torque generated by the PTO system. The torque variations follow a controlled pattern, with the PID system ensuring smoother transitions and avoiding excessive peaks that could lead to mechanical wear or energy losses. The phase relationship between torque and relative velocity remains crucial in maximizing energy conversion, as energy extraction efficiency depends on maintaining a proper phase difference between these variables. Panel B presents the instantaneous power output of the PTO system. While the power generation has increased compared to the uncontrolled case, it remains lower than in the optimal control scenario. This result aligns with fundamental control theory: PID controllers are designed to regulate system stability rather than maximize power output. The trade-off between maintaining structural integrity and optimizing energy extraction explains why the PID-controlled system exhibits moderate

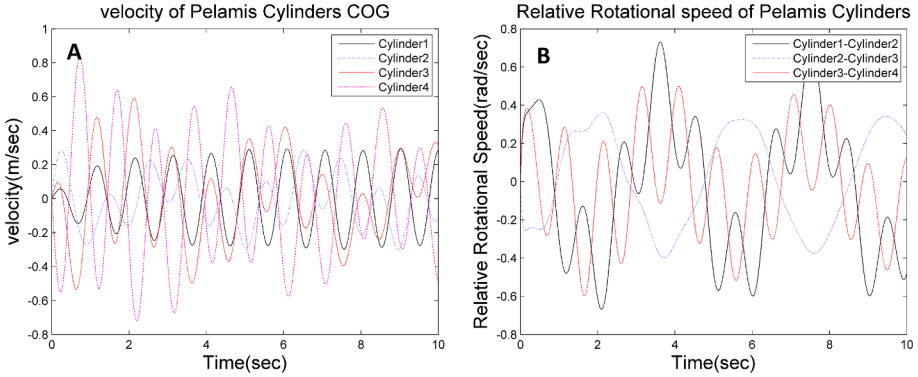


**Fig. 11.** Mass center velocity of Pelamis cylinders (Panel A); relative angular velocity of Pelamis cylinders (Panel B).

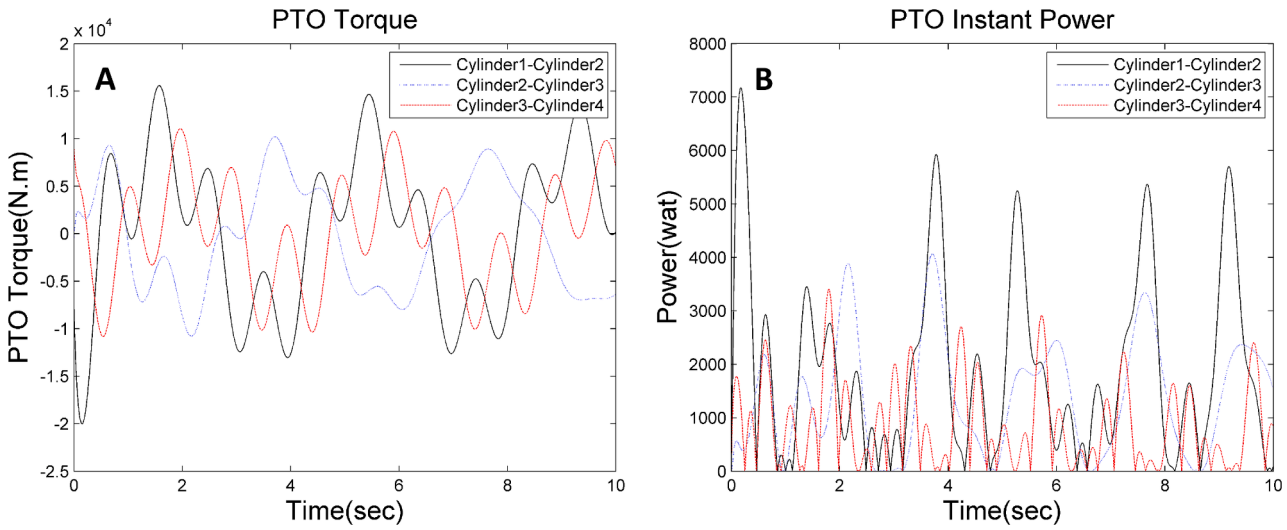


**Fig. 12.** PTO torque calculated by optimal controller (Panel A); instant power generated by PTO systems (Panel B).

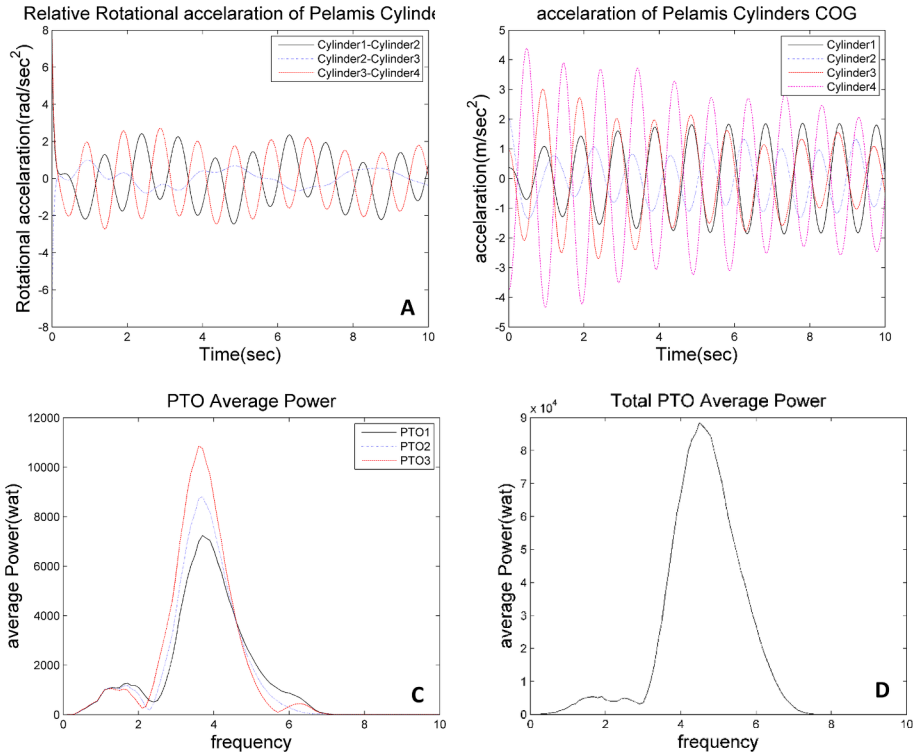


**Fig. 13.** Relative angular acceleration of Pelamis cylinders (Panel A); linear acceleration at the mass center of Pelamis cylinders (Panel B); PTO Average Power generated by the Pelamis (Panel C), and total PTO average power generated by the Pelamis (Panel D).

power improvements over the uncontrolled case.

Fig. 17 provides further insights into the energy conversion process under PID control. Panel A displays the relative angular acceleration of the Pelamis cylinders, showing that oscillatory behavior remains within controlled limits. This is crucial in reducing excessive mechanical stress, which can lead to material fatigue and long-term performance degradation. The controlled acceleration ensures that the energy transfer remains within the operational limits of the mechanical and hydraulic components. Panel B depicts the linear acceleration at the mass center of the cylinders. Unlike the optimal control case, where rapid dynamic adjustments maximize energy absorption, the PID-controlled system exhibits a more moderate acceleration pattern, reflecting its role in stabilizing oscillations. Panels C and D highlight the average power generated by each PTO system and the total PTO average power across the entire Pelamis device. The power-frequency relationship confirms that energy extraction efficiency is wave-frequency-dependent, with peak efficiency occurring at specific resonance conditions. While the total power output is significantly higher than in the uncontrolled case, it remains lower than the optimal control system, demonstrating the fundamental difference between stability-oriented (PID) and energy-maximizing (optimal) control strategies.

The results indicate that while the PID control strategy enhances energy extraction compared to the uncontrolled system, its performance is inherently limited by its primary objective: maintaining system stability rather than maximizing power output. The observed trends align with physical principles governing oscillatory systems, greater

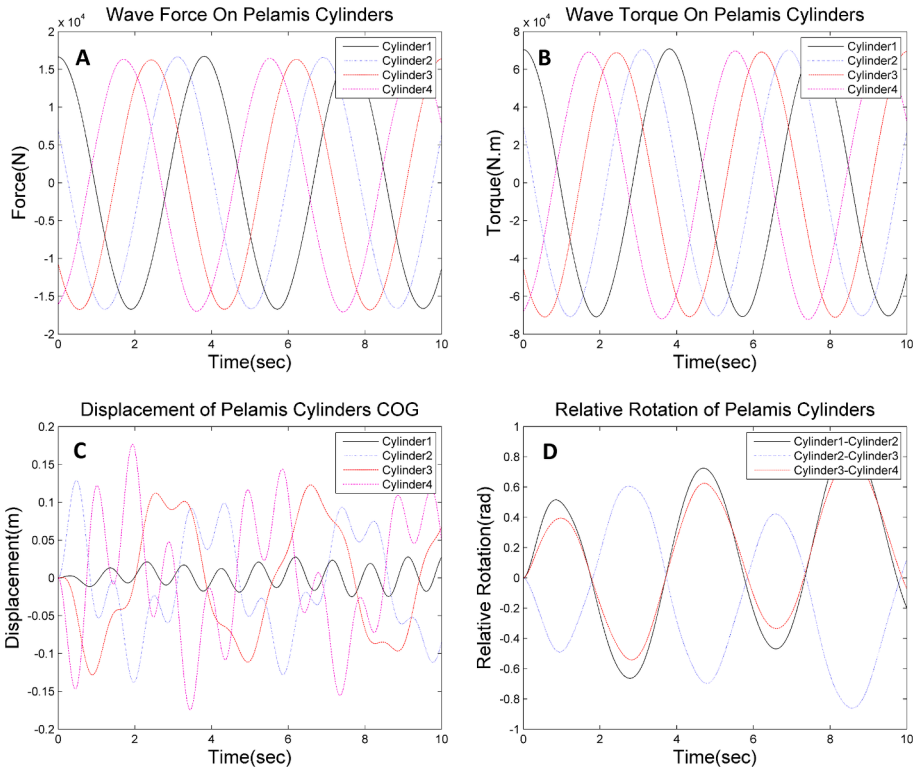


**Fig. 14.** Force applied to the Pelamis cylinders (panel A); moment applied to the Pelamis cylinders (Panel B); displacement of the mass center of Pelamis cylinders (Panel C); and relative angular displacement between the Pelamis cylinders (Panel D).

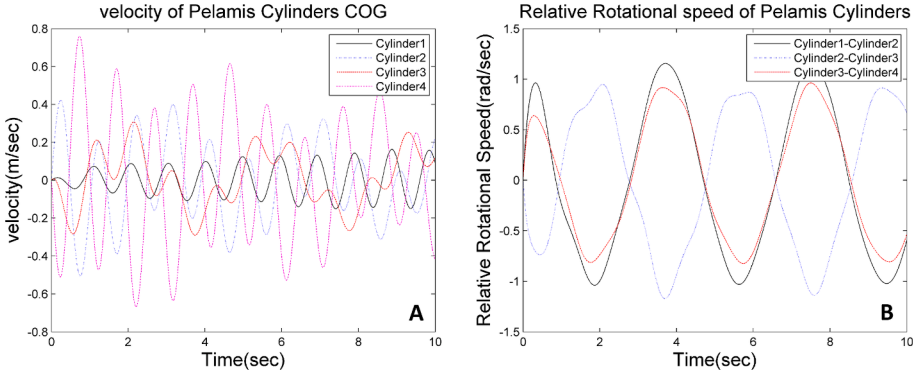


**Fig. 15.** Mass center velocity of Pelamis cylinders (panel A); relative angular velocity of Pelamis cylinders (Panel B).

controlled motion leads to increased energy transfer, but a purely PID-based approach cannot fully exploit the available wave energy.

### *3.4. Comparison of Pelamis performance in controlled and uncontrolled conditions*

Fig. 18 presents a comparative analysis of the total PTO average power under three different operational conditions: without control, with PID control, and with optimal control. The results demonstrate the substantial impact of control strategies on the energy extraction capability of the Pelamis wave energy converter.

In the uncontrolled mode, the PTO system's energy generation is constrained by the fixed hydraulic specifications, which passively respond to wave excitation. Without an active control strategy, the system cannot dynamically adjust to varying wave conditions, leading to suboptimal energy conversion. This is reflected in the low power output observed across all wave frequencies. With the PID control system, the PTO moment is dynamically adjusted, enabling a more efficient utilization of the system's energy extraction capabilities. The PID controller stabilizes the system, preventing excessive oscillations while moderately increasing power generation. The results show that PID control enhances energy production by more than twice that of the uncontrolled mode, as it enables better synchronization of the PTO system with wave-induced motion. The optimal control system significantly outperforms both the PID-controlled and uncontrolled cases. The power generation is amplified up to ten times higher than in the uncontrolled mode, maximizing energy capture from ocean waves. This improvement is attributed to the ability of optimal control to continuously adjust the PTO system's stiffness and damping coefficients, ensuring the system operates in resonance with the incoming waves. This resonance effect leads to larger relative angular velocities and oscillation amplitudes, allowing the system to extract the maximum possible energy while maintaining mechanical constraints.

However, an increase in oscillation amplitudes must be carefully managed to prevent excessive displacement and ensure the system remains within safe operational limits. Thus, while optimal control

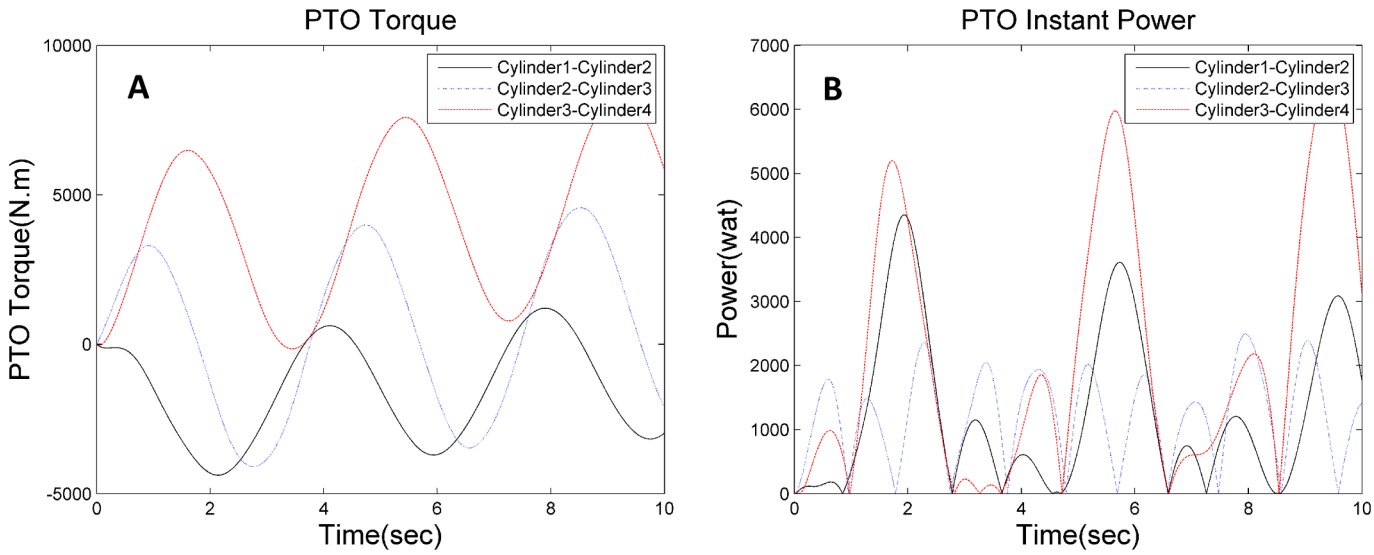


**Fig. 16.** Moment of PTO system calculated by PID controller (Panel A); instant power generated by PTO systems (Panel B).

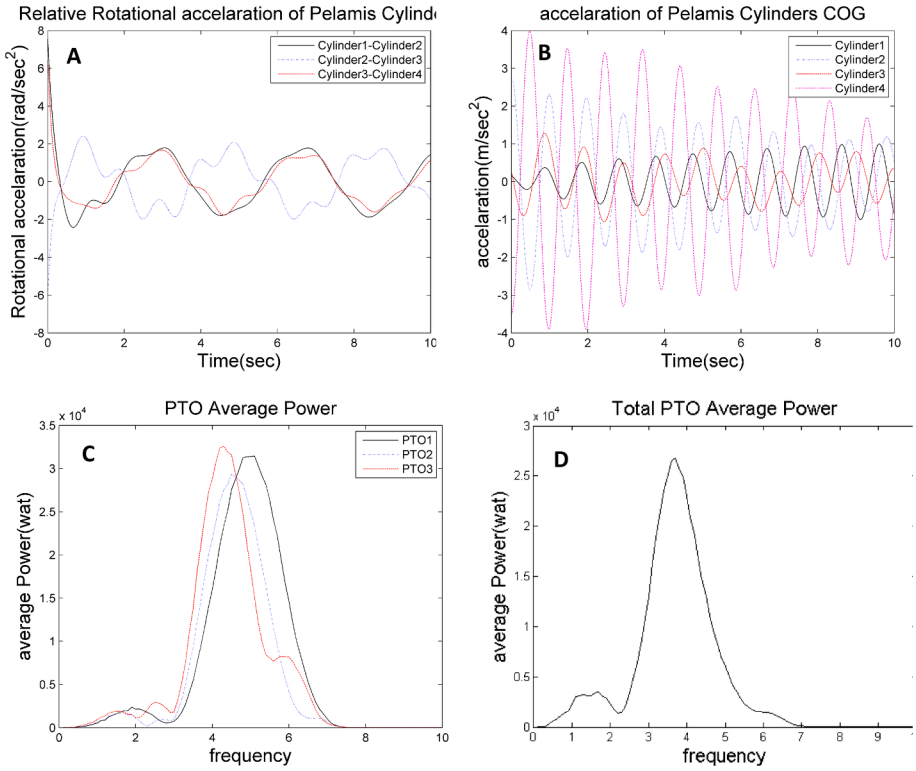


**Fig. 17.** Relative angular acceleration of Pelamis cylinders (Panel A); linear acceleration at the mass center of Pelamis cylinders (Panel B) and PTO Average Power generated by the Pelamis (Panel C); Total PTO Average Power generated by the Pelamis (Panel D).

significantly enhances energy production, careful tuning of control parameters is required to balance energy extraction and system stability. In summary, in uncontrolled mode the power extraction is limited due to fixed PTO parameters, in PID control we observed the moderate power increase (~2×), stabilizing oscillations while improving energy conversion, and finally the maximum power enhancement (~10×)is achieved utilizing the optimal control, leveraging resonance to extract the highest energy yield. This analysis underscores the critical role of advanced control strategies in wave energy converters, demonstrating that optimal control is the most effective approach in maximizing Pelamis' power generation while maintaining structural stability.

## 4. Conclusions

The Pelamis Wave Energy Converter is designed to harness ocean waves' energy. It consists of four cylindrical pods connected by hinge joints and positioned vertically in the sea. The energy extraction mechanism is based on the relative motion of the cylinders at the hinge joints. The optimization of the converter's capacity and the extraction of maximum energy from ocean waves is a key challenge in the design of wave energy converters. This study proposed a solution through a PTO (Power Take-Off) system control for the Pelamis wave energy converter. The dynamics equations that describe the behavior of the Pelamis and its

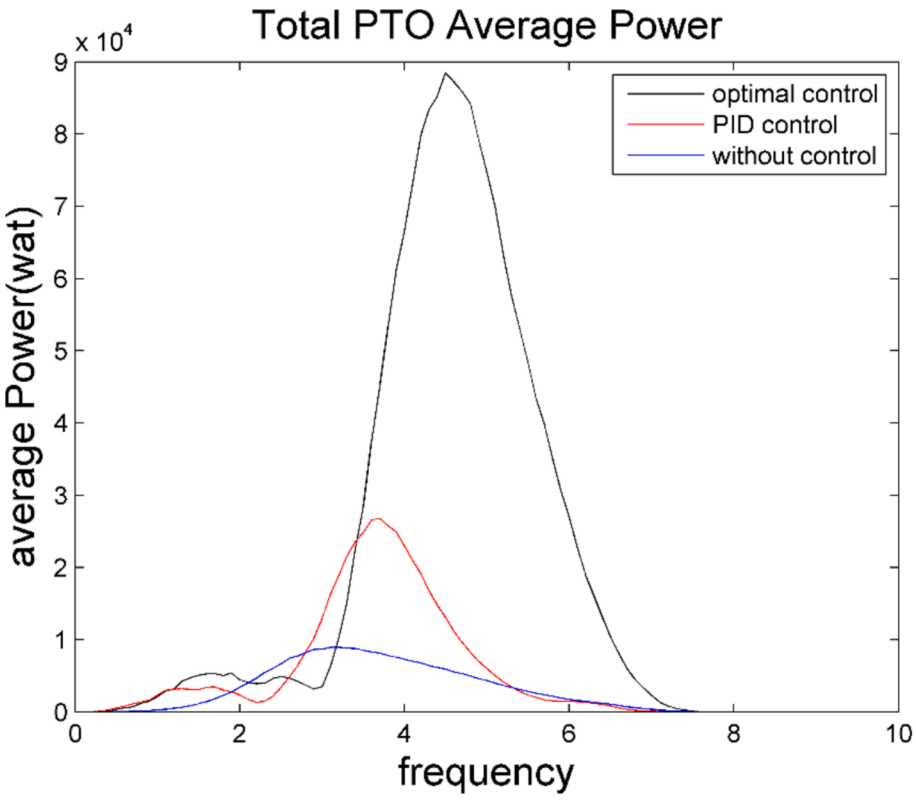


**Fig. 18.** Comparison of Pelamis performance with and without control systems.

interaction with ocean waves were extracted and analyzed, considering the existing constraints posed by the hinge joints. The output torque at the hinge joints was utilized as the control input for the Pelamis, and an optimal control approach was employed to maximize energy extraction and utilize the converter's full capacity. The efficiency of the control method was evaluated through simulation using Simulink software, and the results were compared for both uncontrolled and controlled scenarios.

The proposed optimal control approach incorporates soft displacement constraints by adjusting the weighting coefficients within the control law. These constraints are not strict box constraints but are instead implicitly enforced through the tuning of the control weights in the PTO system. By appropriately selecting these weights, the displacement performed by the wave energy converter can be limited within acceptable ranges to prevent excessive motion and potential damage. This approach allows for flexibility in balancing energy extraction and mechanical safety. Specifically, the control system determines the torque the PTO system generates at any moment, with hydraulic valves dynamically adjusting the equivalent stiffness and damping coefficients of the PTO system to maximize the received energy while maintaining safe operational limits.

The results showed that using the optimal control system significantly increases the energy obtained from the Pelamis. The optimal control system increased the power generation capacity by up to 10 times for all input wave frequencies, while the PID (Proportional-Integral-Derivative) control system increased it by more than two times compared to the uncontrolled case. The average power spectral analysis further indicates that the increase in energy production with the controller is achieved across all wave frequencies. By examining the force and torque graphs in all three uncontrolled and controlled states, it can be observed that applying the control system to the energy converter has resulted in a significant increase in the range of changes in the system's behavior, especially in displacements and rotations. Moreover, by examining the torque graphs generated by the PTO system, which is calculated by the controller, and the relative angular velocity graphs in the controlled states, the generated torque is almost in sync with the relative angular velocity. It acts against it in some parts to prevent excessive physical displacement of the PTO system's cylinders, thereby avoiding damage and destruction to the system. The consideration of soft displacement constraints through optimal control provides a method to regulate the converter's motion while ensuring high energy capture efficiency.

## 5. Uncertainties, limitations and future directions

In this study, several approximations and modeling assumptions introduce inherent uncertainties that may affect the results. While efforts have been made to minimize these uncertainties, we acknowledge that certain simplifications were necessary to ensure computational feasibility and clarity in assessing control strategies for the Pelamis wave energy converter.

Wind-generated waves in real ocean conditions exhibit a random and irregular nature, yet most offshore engineering analyses rely on regular wave approximations [36]. In this study, regular waves are used instead of irregular or stochastic waves to provide a controlled and repeatable environment for evaluating the effectiveness of different control strategies. This approach ensures a clear assessment of the system's dynamic response while minimizing uncertainties associated with wave variability. Furthermore, using regular waves facilitates comparability with prior research [37,38] and enhances computational feasibility by avoiding the complexities of stochastic wave behavior. However, we acknowledge that real-world wave interactions are more complex, and future studies could explore the impact of irregular wave conditions on control performance.

The Pelamis wave energy converter operates in a highly nonlinear ocean environment, where fluid-structure interactions, wave irregularities, and drag forces significantly influence system behavior. However, for this study, a linearized model was adopted to simplify the control

design and evaluation process. The hydrodynamic parameters in the model incorporate nonlinear effects indirectly through equivalent damping and stiffness coefficients derived from hydrodynamic equations. While this approach allows for efficient analysis, future studies could improve model accuracy by incorporating higher-order hydrodynamic models or fully nonlinear wave-structure interaction effects to refine system performance predictions. Furthermore, the proposed method incorporates soft displacement constraints by tuning the weighting coefficients in the control law, which, while effective, does not explicitly enforce strict box constraints. This limitation means that the methodology may not fully address scenarios requiring rigid displacement bounds under extreme wave conditions. Future work should explore the integration of strict constraint-handling techniques to enhance the robustness of the control system.

The cost function (representing the energy extraction performance and is used within the Hamiltonian framework to derive the optimal control law) exploited in this study is designed to evaluate the impact of different control strategies on energy extraction efficiency. While physical constraints such as PTO torque limits, actuator saturation, and mechanical constraints are not explicitly included in the optimization process, these limitations could be integrated into future control strategies to improve real-world applicability. The current framework provides valuable insights into control performance under idealized conditions, but practical implementation would require additional considerations regarding system constraints.

The robustness of the presented results depends on model parameter selections, including hydrodynamic coefficients, PTO system characteristics, and wave conditions. While this study focuses on control strategy evaluation, a comprehensive sensitivity analysis would be a valuable future extension. Such an analysis could quantify the influence of varying model parameters on energy extraction efficiency, providing insights into system adaptability under changing ocean conditions. Future research could explore how parameter variations affect control performance, ensuring the proposed strategies remain effective in real-world applications.

## CRediT authorship contribution statement

**Alireza Vakili:** Writing – review & editing, Writing – original draft, Visualization, Validation, Methodology, Investigation, Formal analysis, Data curation, Conceptualization. **Ali Pourzangbar:** Writing – review & editing, Writing – original draft, Validation, Supervision, Resources, Project administration, Conceptualization. **Mir Mohammad Ettefagh:** Writing – review & editing, Writing – original draft, Supervision, Resources, Project administration, Funding acquisition. **Maghsoud Abdollahi Haghghi:** Conceptualization, Writing – review & editing, Investigation.

## Declaration of competing interest

The authors declare that they have no known competing financial interests or personal relationships that could have appeared to influence the work reported in this paper.

## Appendix A. Supplementary data

Supplementary data to this article can be found online at https://doi.org/10.1016/j.ref.2025.100685.

## Data availability

No data was used for the research described in the article.

## References


[1] Y. Zhang, Y. Zhao, W. Sun, J. Li, Ocean wave energy converters: technical principle, device realization, and performance evaluation, Renew. Sustain. Energy Rev. 141 (2021) 110764.

[2] J. Cruz, Ocean wave energy: current status and future perspectives, Springer Science & Business Media (2007), https://doi.org/10.1016/j.rser.2021.110764.

[3] A.F.D.O. Falcão, Wave energy utilization: a review of the technologies, Renew. Sustain. Energy Rev. 14 (3) (2010) 899–918, https://doi.org/10.1016/j.rser.2009.11.003.

[4] O. Langhamer, K. Haikonen, J. Sundberg, Wave power—sustainable energy or environmentally costly? A review with special emphasis on linear wave energy converters, Renew. Sustain. Energy Rev. 14 (4) (2010) 1329–1335, https://doi.org/10.1016/j.rser.2009.11.016.

[5] M. Al Karim, Assessment of a simplified model of a wave energy converter in terms of hydraulic mechanical and electrical parameters, International Journal of Energy and Power Engineering 4 (2015), https://doi.org/10.11648/j.ijepe.20150402.20.

[6] A. Pourzangbar, A. Vakili, Research priorities given the MRE converters: a case study in Wales. in: 14th International Conference on Coasts, Ports and Marine Structures, 2022.

[7] B. Czech, P. Bauer, Wave energy converter concepts: Design challenges and classification. IEEE Industrial Electronics Magazine 6(2) 2012, 4-16. https://doi: 10.1109/MIE.2012.2193290.

[8] M.D. Esteban, J.S. López-Gutiérrez, V. Negro, M. Laviña, P. Muñoz-Sánchez, A new classification of wave energy converters used for selection of devices, J. Coast. Res. 85 (2018) 1286–1290, https://doi.org/10.2112/SI85-258.1.

[9] G.J. Dalton, R. Alcorn, T. Lewis, Case study feasibility analysis of the Pelamis wave energy converter in Ireland, Portugal and North America, Renew. Energy 35 (2) (2010) 443–455, https://doi.org/10.1016/j.renene.2009.07.003.

[10] M.H. Jahangir, R. Alimohamadi, M. Montazeri, Performance comparison of pelamis, wavestar, langley, oscillating water column, and aqua buoy wave energy converters supplying islands' energy demands, Energy Rep. 9 (2023) 5111–5124, https://doi.org/10.1016/j.egyr.2023.04.051.

[11] R. Henderson, Design, simulation, and testing of a novel hydraulic power take-off system for the Pelamis wave energy converter, Renew. Energy 31 (2) (2006) 271–283, https://doi.org/10.1016/j.renene.2005.08.021.

[12] M. O'Connor, T. Lewis, G. Dalton, Techno-economic performance of the Pelamis P1 and Wavestar at different ratings and various locations in Europe, Renew Energy 50 (2013) 889–900, https://doi.org/10.1016/J.RENENE.2012.08.009.

[13] R.C. Thomson, J.P. Chick, G.P. Harrison, An LCA of the Pelamis wave energy converter, Int. J. Life Cycle Assess. 24 (1) (2019) 51–63, https://doi.org/10.1007/s11367-018-1504-2.

[14] D.T. Johnson, G. Martinez, Environmental impact assessment of wave energy converters: a case study on offshore deployments, Mar Policy 143 (2022) 104738, https://doi.org/10.1016/j.marpol.2022.104738.

[15] H. Ghaneei, M. Mahmoudi, Simulation, optimization, and economic assessment of pelamis wave energy converter, J. Ocean Technol. 17 (2022), https://doi.org/10.2139/ssrn.3939656.

[16] A. Ghaedi, R. Sedaghati, M. Mahmoudian, S. Bazyari, Reliability modeling of wave energy converters based on Pelamis technology, Electr. Pow. Syst. Res. 227 (2024) 109977, https://doi.org/10.1016/j.epsr.2023.109977.

[17] N. Faedo, G. Giorgi, G. Mattiazzo, J.V. Ringwood, Nonlinear moment-based optimal control of wave energy converters with non-ideal power take-off systems, in: Proceedings of the International Conference on Offshore Mechanics and Arctic Engineering -, 2022, https://doi.org/10.1115/OMAE2022-81267.

[18] L.G. Wang, P.Y. Hu, W.C. Chen, F. Feng, Enhanced energy harvesting of wave energy converters in site-specific wave climates: a hybrid approach by geometric shape optimization and power take-off control, Ocean Eng. 257 (2022) 111553, https://doi.org/10.1016/J.OCEANENG.2022.111553.

[19] G.O.G. Avalos, M. Shadman, S.F. Estefen, Application of the latching control system on the power performance of a wave energy converter characterized by gearbox, flywheel, and electrical generator, J. Mar. Sci. Appl. 20 (2021), https://doi.org/10.1007/s11804-021-00238-7.

[20] T. Demonte Gonzalez, G.G. Parker, E. Anderlini, W.W. Weaver, Sliding mode control of a nonlinear wave energy converter model, J Mar Sci Eng 9 (2021), https://doi.org/10.3390/jmse9090951.

[21] A.F. de Falcão, Phase control through load control of oscillating-body wave energy converters with hydraulic PTO system, Ocean Eng. 35 (2008) 358–366, https://doi.org/10.1016/J.OCEANENG.2007.10.005.

[22] W. Ni, X. Zhang, W. Zhang, S. Liang, Numerical investigation of adaptive damping control for raft-type wave energy converters, Renew Energy 175 (2021) 520–531, https://doi.org/10.1016/J.RENENE.2021.04.128.

[23] Z. Nizamani, L.L. Na, A. Nakayama, M.O.A. Ali, M.A. Nizamani, Renewable wave energy potential for the sustainable offshore oil platforms in South China Sea, IEEE Access 9 (2021) 116973–116993, https://doi.org/10.1109/ACCESS.2021.3104729.

[24] S. Sheshaprasad, F. Naghavi, S. Hasanpour, M. Albader, M.C. Gardner, H.Y. Kang, H.A. Toliyat, Optimal Electric Power Take-off Strategy for Surface Riding Wave Energy Converter, in: 2022 IEEE Energy Conversion Congress and Exposition 2022, ECCE 2022. DOI: 10.1109/ECCE50734.2022.9947696.

[25] L.G. Wang, T. Zhao, M.F. Lin, H. Li, Towards realistic power performance and techno-economic performance of wave power farms: the impact of control strategies and wave climates, Ocean Eng. 248 (2022) 110754, https://doi.org/10.1016/J.OCEANENG.2022.11.

[26] A.F. de Falcão, J.C.C. Henriques, L.M.C. Gato, Adaptive control strategies for optimizing energy harvesting in irregular wave conditions, Renew Energy 210 (2023) 10–20, https://doi.org/10.1016/j.renene.2023.03.045.
[27] H. Mehdipour, E. Amini, S.T.O. Naeeni, M. Neshat, A.H. Gandomi, Optimization of power take-off system settings and regional site selection procedure for a wave energy converter, Energy Convers. Manage.: X 22 (2024) 100559, https://doi.org/10.1016/j.ecmx.2024.100559.
[28] C. Hall, W. Sheng, Y. Wu, G. Aggidis, The impact of model predictive control structures and constraints on a wave energy converter with hydraulic power take off system, Renew. Energy 224 (2024) 120172, https://doi.org/10.1016/j.renene.2024.120172.
[29] X. Shao, J.W. Ringsberg, H.D. Yao, E. Johnson, J. Forsberg, S. Zeinali, M. Wiktorsson, A comparison of approaches integrating power take-off systems into wave energy converters simulations, in: Innovations in Renewable Energies Offshore, CRC Press, 2024, pp. 351–358.
[30] R. Ali, M. Meek, B. Robertson, Submerged wave energy converter dynamics and the impact of PTO-mooring configuration on power performance, Renew. Energy 122525 (2025), https://doi.org/10.1016/j.renene.2025.122525.
[31] M. Aghanezhad, R. Shafaghat, R. Alamian, S.M.A. Seyedi, M.J.R. Asadabadi, Experimental study on performance assessment of hydraulic power take-off system in centipede wave energy converter considering caspian sea wave characteristics, Int. J. Eng. Trans. B 35 (2022), https://doi.org/10.5829/ije.2022.35.05b.05.
[32] T.C. Do, T.D. Dang, K.K. Ahn, Efficiency improvement of a hydraulic power take-off of wave energy converter using variable displacement motor, International Journal of Precision Engineering and Manufacturing - Green Technology 9 (2022), https://doi.org/10.1007/s40684-021-00371-2.
[33] J. Tan, H. Polinder, A.J. Laguna, S. Miedema, The application of the spectral domain modeling to the power take-off sizing of heaving wave energy converters, Appl. Ocean Res. 122 (2022) 103110, https://doi.org/10.1016/J.APOR.2022.103110.
[34] N.E. Andersen, J.B. Mathiasen, M.G. Carøe, C. Chen, C.E. Helver, A.L. Ludvigsen, N. F. Ebsen, A.H. Hansen, Optimisation of control algorithm for hydraulic power take-off system in wave energy converter, Energies (Basel) 15 (2022) 1–18, https://doi.org/10.3390/en15197084.
[35] M.G. Veurink, W.W. Weaver, R.D. Robinett, D.G. Wilson, R.C. Matthews, WEC array optimization with multi-resonance and phase control of electrical power take-off, IFAC-PapersOnLine 55 (2022) 1–6, https://doi.org/10.1016/J.IFACOL.2022.10.479.
[36] Y. Goda, Random seas and design of maritime structures. Advanced series on ocean engineering Vol. 15 (2010), https://doi.org/10.1142/7425.
[37] A. Madaghalechi, Fault detection of pelamis wave converter system using dynamic response signal, Tabriz University, 2015.
[38] F. Paparella, J.V. Ringwood, Optimal control of a three-body hinge-barge wave energy device using pseudospectral methods, IEEE Trans. Sustainable Energy 8 (2017) 200–207, https://doi.org/10.1109/TSTE.2016.2592099.
[39] J.V. Ringwood, G. Bacelli, F. Fusco, Energy-maximizing control of wave-energy converters: the development of control system technology to optimize their operation, IEEE Control Syst 34 (2014), https://doi.org/10.1109/MCS.2014.2333253.
[40] A. Preumont, Vibration Control of Active Structures: An Introduction, 3rd ed., Springer, Netherlands, 2011.
[41] A. Borzì, The Sequential Quadratic Hamiltonian Method: Solving Optimal Control Problems 2021. CRC Press. ISBN: 978-0367715526.
[42] B.D.O. Anderson, J.B. Moore, Optimal Control: Linear Quadratic Methods, Dover Publications, 2007.